

3.1 THUNDERSTORM NOWCASTING AND CLIMATOLOGY USING CYLINDRICAL COORDINATE HOVMÖLLER DIAGRAMS: AN NLDN APPLICATION

Thomas A. Seliga^{1*} and David A. Hazen²

1. Volpe National Transportation Systems Center, Cambridge, MA
2. Titan/System Resources Corporation, Billerica, MA

1. INTRODUCTION

This paper demonstrates the potential utility of using cylindrical coordinate Hovmöller diagrams, also known as polar Hovmöller diagrams, for examining the behavior and spatial characteristics of lightning flashes during thunderstorms near airports (or other points of interest). There are two diagrams per location and time interval. One diagram plots lightning flash density with time proceeding downwards on the Y-axis and distance from the location or point of interest on the X-axis. The other diagram similarly plots lightning flash density, except with the X-axis representing the azimuthal angular direction relative to true North.

The lightning data used here were obtained from archived reports on lightning cloud-to-ground flashes reported by Global Atmospheric, Inc. (GAI) through its National Lightning Detection Network (NLDN). The NLDN detects and reports the occurrence of cloud-to-ground lightning flashes throughout the CONUS (Orville, 1991; Orville and Silver, 1997; Orville and Huffines, 1999; Orville and Huffines, 2001). The lightning data that are represented on distance vs time plots or Hovmöller diagrams in this paper are analyzed similarly to lat/long plots reported in previous studies (Seliga et al., 2002a, b). The study introduces polar Hovmöller diagrams, which consist of one plot of distance vs. time and another plot of azimuth angle vs. time. These Hovmöller plots have a spatial resolution of 1-nm in radius and 5° in azimuth angle and a temporal resolution of 10 min. Lightning flash counts are plotted using a log scale on all plots in this paper in order to capture the dynamic range of events. Plots of weekly, monthly and seasonal averages are included to show spatial and temporal flash distributions relative to selected sites behave climatologically. Case studies of lightning activity in the vicinity of Chicago/O'Hare International Airport (ORD) and George Bush Intercontinental Airport/Houston (IAH) are discussed.

2. PREVIOUS STUDIES

The U.S. DOT Volpe Center has utilized and analyzed NLDN data for over 13 years, primarily in support of the FAA's program to automate the detection and reporting of thunderstorms through Automated Weather Observing Systems (AWOS) and Automated Surface Observing Systems (ASOS) (Canniff, 1993; Kraus and Canniff, 1995; Kraus et al., 2000; Seliga and Shorter, 2000). Essentially, NLDN data signify the occurrence of

cloud-to-ground lightning flashes and represent the occurrence of thunderstorms throughout the U.S. The data have proven useful for numerous applications and investigations (e.g., Changnon, 1988a, b; Holle and Lopez, 1993; Orville, 1991; Orville and Silver, 1997; Orville and Huffines, 1999; Rhoda and Pawlak, 1999; Seliga and Shorter, 2000; Orville and Huffines, 2001; Bates et al., 2001).

The NLDN flash data examined here cover the summer of 2003 time period, which represents a major period of thunderstorm activity. All times are in Greenwich Mean Time (GMT). Conversion to local (Central Daylight Savings Time) time requires subtracting 5 hrs from GMT.

3. POLAR HOVMÖLLER DIAGRAMS

The lightning data presented here are examined using a variation of the time-distance Hovmöller diagrams introduced by Carbone et al. (2002) for analyzing NEXRAD data for warm season storm characterizations over a large portion of the CONUS and then by Seliga et al. (2002a) using NLDN lightning data. The applicable time scales can range from hours to days to months to seasons to years. Such diagrams have been found useful for gleaning properties of weather activity as well as for climatological studies that examine interrelationships among one or more variables such as rainfall, temperature and winds. The diagrams used in Seliga et al. (2002a, b) are latitudinal and longitudinal Hovmöller plots of NLDN data. The latitude and longitude Hovmöller diagrams are, however, deficient in their ability to relate directly to a specific location such as, for example, a town or city and an airport or other transportation node. The polar plots indicate where (the range and direction from which) and when (time history) storms are approaching or receding from the point of interest. On the other hand, latitude and longitude diagrams provide information relative to the designated latitudinal or longitudinal lines of interest. The plots are introduced using data from one-day events at IAH and ORD. Plots of lightning activity averaged over periods of one-week, one-month and one-season illustrate general weather and climatic behavior relative to these airport locations.

Figs. 1 and 2 show the lightning activity within 120 nm of IAH for June 4, 2003. Fig. 1 plots lightning activity as functions of distance (nm) and time (GMT) while Fig. 2 plots lightning activity as functions of azimuth angle and

* Corresponding Author Address: Thomas A. Seliga, Surveillance and Assessment Division, DTS-53, Volpe National Transportation Systems Center, 55 Broadway, Cambridge, MA 02142-1093; **Email:** seliga@volpe.dot.gov

time. The flash occurrence plots are normalized by areal range rings of 1-nm width and are plotted using a logarithmic scale. That is, the image plot is given by

$$L_S = 10 \log_{10}(L + 1) \quad (1)$$

where L is the number of flashes occurring in any 10-min time interval and L_S is its corresponding logarithmically-scaled value. Other choices of a metric for lightning activity can be selected. This one provides a uniform normalization to spatial area and the logarithmic transformation allows a larger range of activity to be plotted. Because storms tend to be dominated by non-uniformity in space, when storms approach the point of interest, L (and L_S) will tend to show greater intensity due to the fact that larger portions of the space covered by equal increments of radial rings will tend to be affected by the presence of a storm than when the same storm is more distant. Another option (not presented here) would be to select an initial circular area centered on the point of interest and then alter the step size of the range bins so as to keep the areal coverage at different distances equal to this same area. This choice would require that the range bins be inversely proportional to range. Even in this case, the tendency of storms to be localized in space will typically cause the range plots to reduce in intensity as range is increased. In either case, the representations will tend to enhance activity as the storms approach the point of interest; this should be a desirable trait for most applications, since it heightens user attention to storms nearer the point of interest. Note that the azimuthal plots behave oppositely as storms approach the point of interest. In this case, the fixed azimuthal sector most often intercepts smaller and smaller portions of a storm as the storm approaches, while farther out the same sector would encompass more and more of the storm. These traits need to be kept in mind whenever cylindrical representations of Hovmöller diagrams are used.

Detailed meteorological interpretation of the data in Figs. 1 and 2 is outside the scope of this study. Nonetheless, a number of features of this day's lightning (thunderstorm) behavior can be readily identified, particularly when accompanied by sample images of the spatial distribution of activity to disclose otherwise irresolvable features in the Hovmöller plots. These features include, for example, storm onset and termination times; storm location at onset and termination; storm duration or persistence as coherent entities and as functions of distance and azimuth angle; storm extent; storm development; storm motion (radial and angular velocities); storm features; and the relative intensity of such features along with intensification and dissipation traits. If sets of azimuth angle Hovmöller plots are generated for flashes occurring within different sub-ranges or range bins, storm components can be resolved more precisely. Plots generated from data gathered over consecutive days (not shown) can be used to detect diurnal patterns and long-term stability or coherency trends relative to a point in space as

opposed to a line for latitudinal-longitudinal plots (Carbone et al., 2002; Seliga et al., 2002a).

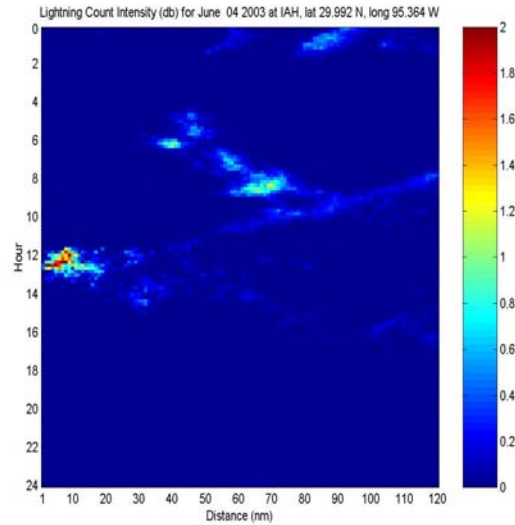


Fig.1. Sample lightning flash polar Hovmöller diagram/plot (time vs. radial distance): George Bush Intercontinental Airport/Houston (IAH) on June 4, 2003.

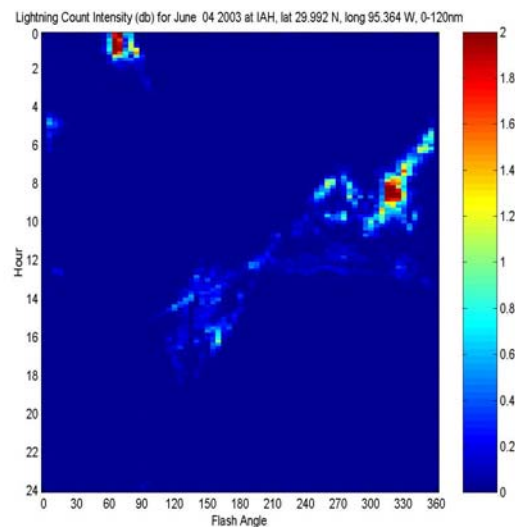


Fig.2. Sample lightning flash polar Hovmöller diagram/plot (time vs. azimuth angle):IAH for June 4, 2003.

Between ~0000-0200, Fig. 1 shows most lightning activity occurred over an extended range from 50-120 nm; these resided in three distinct range bands (50-65 nm; 77-100 nm; 102-120 nm). The second range band was somewhat more intense and organized than the first and third range bands. This same time period in the corresponding azimuth Hovmöller diagram given in Fig. 2 shows that this activity was confined to a relatively narrow ENE sector. Fig. 1 showed dissipation from ~0120-0200. New activity formed to the north at a distance of ~45 nm of IAH just after 0400, which then extended both towards and away from IAH, coming as

close as ~30 nm by ~0620. The activity started N-NNE of IAH, then veered to N and then continued to NW by ~0800. The activity had intensity peaks at ~0440 and ~0520. All the activity in this domain then moved away from IAH and dissipated by ~0630. More intense activity formed starting at ~0620 from the W but never came nearer than ~50 nm of IAH. The most significant feature of Fig.1 is the steady approach of activity from 120 nm out at ~0750 to ~1 nm by ~1230 with varying intensity. The intensity was light to moderate from ~0800-1010 while the activity moved from ~120 nm to ~70 nm of IAH. The activity was to the W and NW of IAH. In the meantime, there was another area that formed at ~70 nm range, intensified, expanded to a maximum range extent of ~50-75 nm at ~0850, then dissipated and merged into the other line while at ~70-80nm range at ~0920. There was a relative lull between ~1100-1150 while moving from ~50 to ~27 nm of IAH; activity then reintensified by ~1140 over a range of ~10 to 30 nm. The storm system then approached IAH from the W and encompassed the area around the airport. The major activity lasted until ~1250 with remnants lasting out to ~1300. The activity then receded towards the SE-S and lessened considerably in intensity for the next several hours. This reduction in activity was accompanied by storm spreading as seen in Fig. 2.

3.1 Average Hovmöller Diagrams

Hovmöller diagrams of averaged data are also useful for determining features of storms and general patterns in the region of interest. All distance Hovmöller plots in this paper are normalized to the area of the annulus defined by the outer radius of each range band. All azimuth angle plots are normalized to the area of sector of interest. These diagrams plot the lightning flash activity for an average day within the week, month or season of interest at resolution sizes of 1-nm radial distance, 5° azimuth angle and 10-min time duration. Diagrams are shown for IAH and ORD.

IAH – Figs.3 and 4 are average Hovmöller plots for the summer of 2003 (June-August). Averaging is achieved by dividing the total lightning flash counts in an area of interest by the number of days included in the data set. The logarithmic transformation is applied after the averaging is performed. Figs. 5 and 6 are average Hovmöller plots of lightning flash data for the month of June 2003 at IAH. Similarly, Figs. 7-8 are plots for the week of June 11-17, 2003 at IAH, which was the week of highest lightning activity of the month of June 2003 at IAH. A number of characteristics of storms in this region can be readily gleaned from these representations.

Storm Occurrence - Fig. 3 shows that the region out to 120-nm from IAH exhibited lightning activity throughout the entire day, although there is a definitive period of time that is devoid of activity within around 50-nm between ~0300 to 1600 (except for the one storm that occurred on June 4 and reached IAH at ~1200; see Fig.1). The plot also shows that the most intense storm activity occurred between ~1600 to 0200. Fig. 3 also shows that the most likely times that storms were within ~3 nm or less of IAH were at ~0040, ~1240, ~1820 and

~2100 during the summer of 2003 with the greatest average intensity occurring at ~1820.

Storm Motion - Fig. 3 shows that most storms remain coherent over durations of ~1-7 hrs and approach or leave the area of interest over practically all sectors. There is a tendency for the dominant late afternoon and evening storms to reside throughout NNE to ESE and SSW to WNW sectors. The strongest azimuthal track started from the N in the early morning at ~1030 and shifted to the W by noontime at ~1700 with an average angular speed of ~14° hr⁻¹. Other tracks have angular speeds typically between ~0-40° per hour.

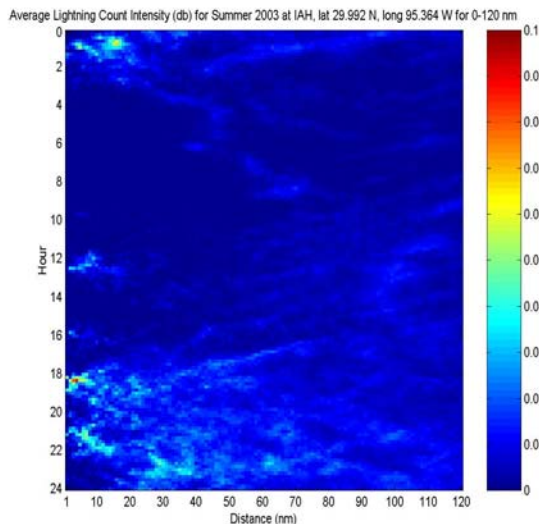


Fig. 3. Hovmöller distance diagram of summer 2003 average flashes at IAH.

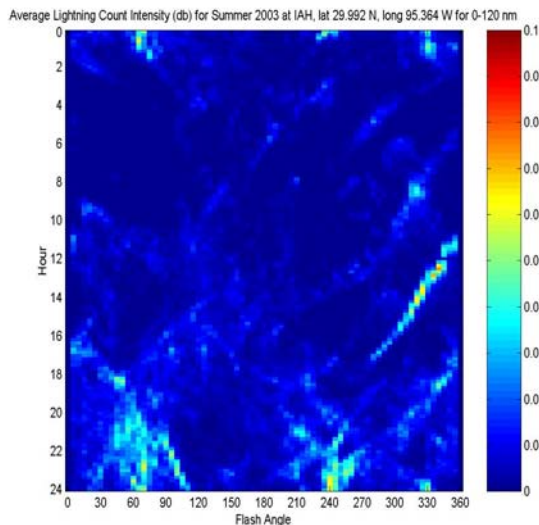


Fig. 4. Hovmöller azimuth angle diagram of summer 2003 average flashes at IAH.

Diurnal Pattern Figs. 3, 5 and 7 exhibit the expected strong diurnal pattern associated with convection arising in response to solar heating. That is, most lightning activity occurred beginning shortly after noon (~1700)

and lasted on through the evening hours. The least activity occurred during the early morning hours (~0300-1600). Fig. 4 shows that the average intensity near IAH (~10 nm range or less) is strongest during the afternoon and evening hours with a peak at ~1820 most evident. For example, thunderstorm initiation typically begins in the early afternoon local time (~1800), peaks in the late afternoon and ends ~0300 the next day. Occasionally, storm tracks are seen to extend on through the morning lull, but are generally distant (> ~50-nm). The angle Hovmöller plots shown in Figs. 4 and 6 show least angular extent and average intensity during late night and pre-dawn hours. Figs 4, 6 and 8 show the least angular extent in the pre-dawn hours and maximum extent and intensity in the afternoon and evening.

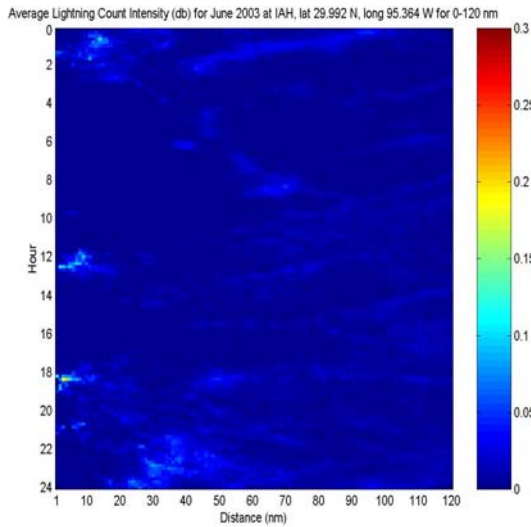


Fig. 5. Hovmöller distance diagram of June 2003 average flashes at IAH.

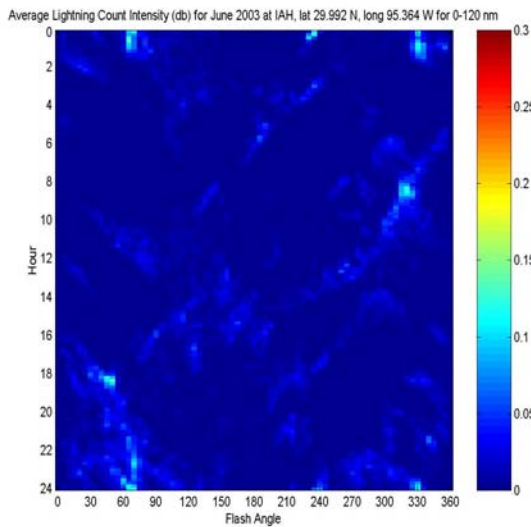


Fig. 6. Hovmöller azimuth angle diagram of June 2003 average flashes at IAH.

Figs. 5 through 8 provide insights into what portion of the plots for the entire summer were derived from the storm activity occurring during the month of June and one week in this month. These plots confirm the previous interpretations such as times of storm occurrence, duration and motion. They combine with Figs. 1 and 2 to demonstrate the hierarchy of plots that can be generated to represent lightning/thunderstorm activity centered on IAH during the summer of 2003.

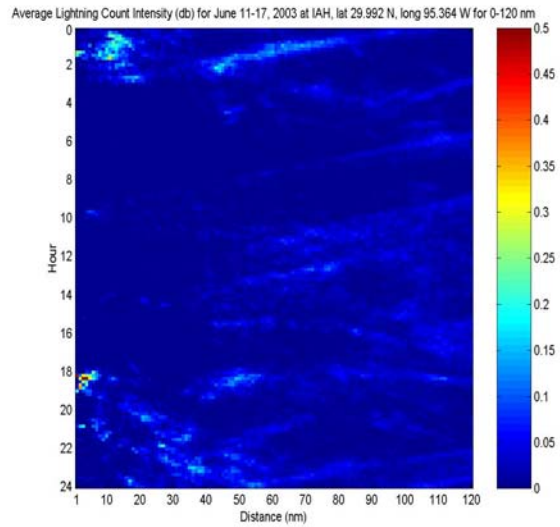


Fig. 7. Hovmöller distance diagram of June 11-17 2003 average flashes at IAH.

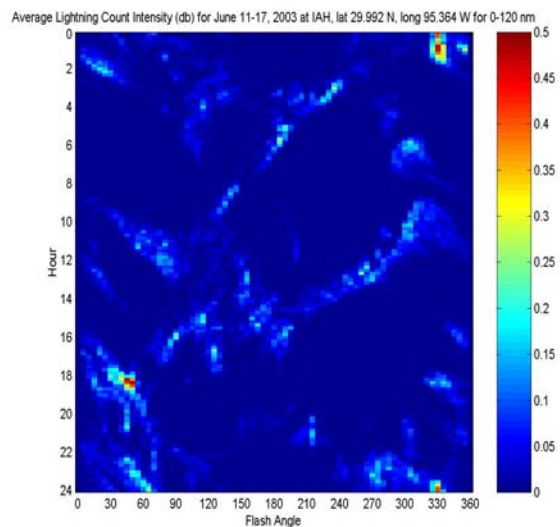


Fig. 8. Hovmöller azimuth angle diagram of June 11-17 2003 average flashes at IAH.

ORD – Figs. 9 and 10 are distance and azimuth angle Hovmöller plots of an average day in the summer of 2003 at ORD, respectively. Figs. 11 and 12 are distance and azimuth angle plots of an average day in July 2003 at ORD, respectively. Figs. 13 and 14 are

distance and azimuth angle plots of an average day for the week of July 4-10, 2003 at ORD, respectively.

Storm Tracks - Fig. 9 shows that many individual storm tracks came within ~5-nm of ORD in the afternoon and evening hours with approaches in the late evening and the most intense average activity in the pre-dawn hours. There is considerable variation in storm radial velocities towards and away from ORD with 30 kts being fairly typical. Fig. 10 shows the activity most concentrated in the late evening and early morning hours with the latter being concentrated mostly in the pre-dawn hours. Storm tracks are again very evident, with durations of several hours typical and angular velocities varying considerably with rates of ~10-30° hr⁻¹ quite common.

in the summer plots. Comparisons with Figs. 9 and 10 indicate strong similarity, evidence that most of the summer storms occurred during July. Further, Figs. 13 and 14 show that the week of July 4-10 dominated activity in July.

Diurnal Pattern - The plots reveal that the diurnal pattern of lightning, except for the presence of early mid-morning storms ~0800-1000, is weaker in the morning hours and increases in the afternoon and evening. Approach and recession speeds are similar for most storms. Figs. 10 and 12 indicate that the most intense activity tends to occur in the SE and SW quadrants, especially from ~0000-1200. At other times, the storms tend to be more westerly of ORD.

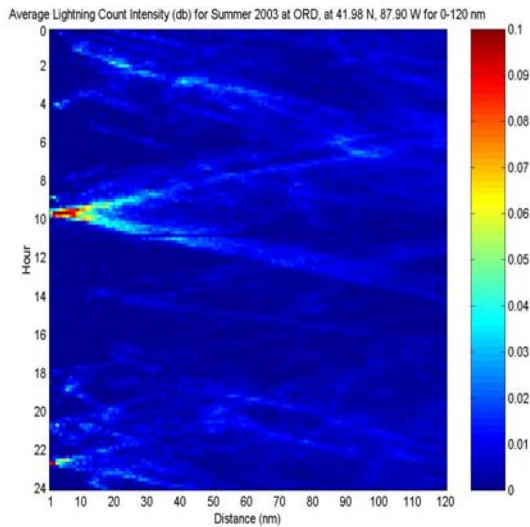


Fig. 9. Hovmöller distance diagram of summer 2003 average flashes at ORD.

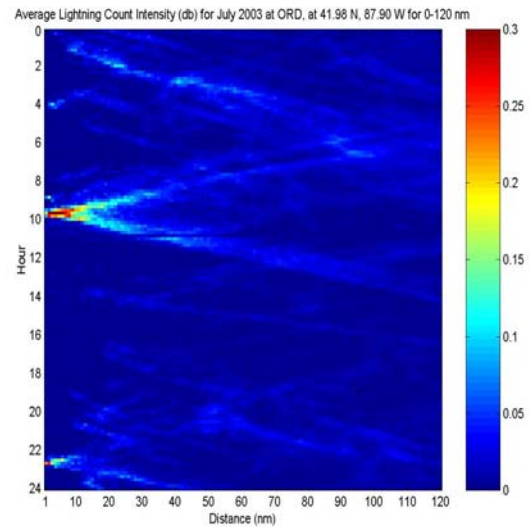


Fig. 11. Hovmöller distance diagram of July 2003 average flashes at ORD.

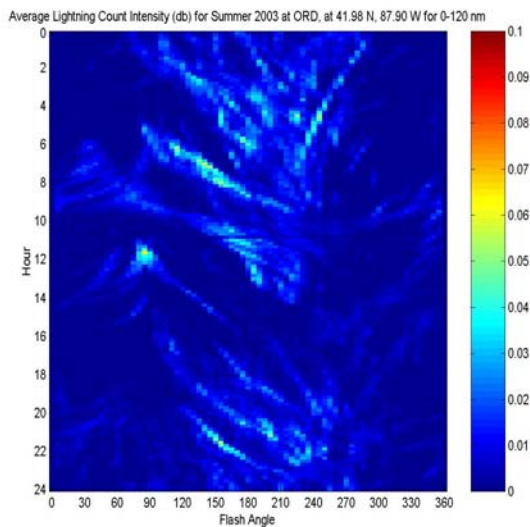


Fig. 10. Hovmöller azimuth angle diagram of summer 2003 average flashes at ORD.

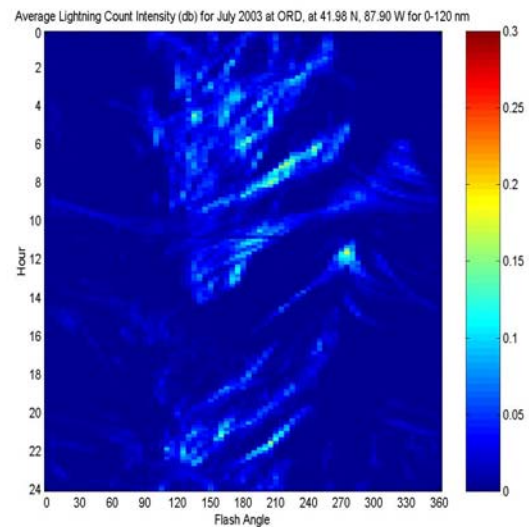


Fig. 12. Hovmöller azimuth angle diagram of July 2003 average flashes at ORD.

The average daily activity plots for July in Figs. 11 and 12 confirm the times and characteristics that are evident

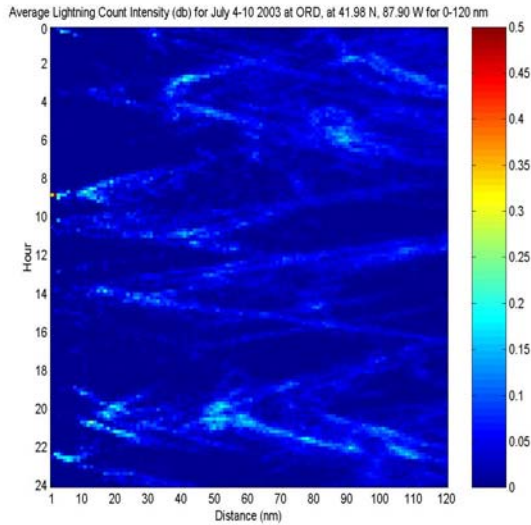


Fig. 13. Hovmöller distance plot of average flashes at ORD, July 4-10, 2003.

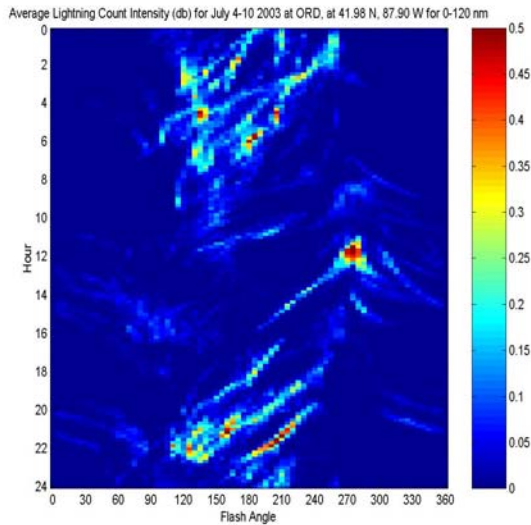


Fig. 14. Hovmöller azimuth angle plot of average flashes at ORD, July 4-10, 2003.

4. CASE STUDIES

This section presents case studies of activity recorded on two select days of high lightning flash activity in July 2003 at ORD and June 2003 at IAH. The daily plots consist of radial distance Hovmöller plots for 0-120-nm along with angle plots for 0-30-nm, 30-60-nm and 60-120-nm ranges. The latter are useful for discriminating locations of coherent storm structures.

4.1 ORD

Fig 15 is a distance Hovmöller plot of lightning activity within 120-nm of ORD on July 6, 2003, which was the Sunday after the Independence Day holiday. Considerable lightning flash activity was experienced near ORD that day. Figs. 16-18 are azimuth angle plots for the same time period. Fig. 16 shows the angle

distribution for flashes 0-30-nm away from ORD; Fig. 17 is for flashes between 30-60-nm; and Fig. 18 is for 60-120-nm.

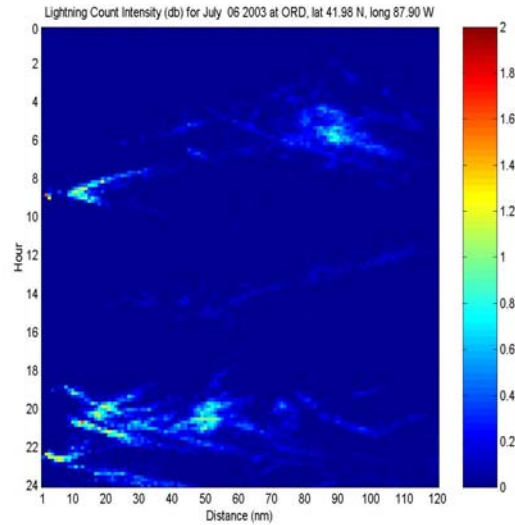


Fig. 15. Distance Hovmöller plot of lightning flashes at ORD on July 6, 2003.

Figs. 15 and 18 shows that the first activity of the day began to the S with very light activity at ~88-100-nm range at ~0200. Possibly as much as seven coherent structures can be seen, indicating that the activity over the range from ~75-110-nm consisted of different individual storms. The motion of these structures was generally similar, having begun mostly to the S, then appearing to rotate counterclockwise or move easterly at similar rates. The most intense activity at these distances developed at a range of ~90 nm at ~0500 in the SSW, which then extended out to ~87-98 nm range at ~0630; after this time the activity lessened considerably. During its lifetime, the activity continued to spread inward and outward as well as intensify so that lightning flashes were occurring in the ~40-120-nm range by ~0600. The area of intense activity receded somewhat from ~0600-0700 while the angular extent shrunk to the SE and S sectors. This area then dissipated to scattered activity in the S and SE sectors from ~0700-0900. Fig. 15 shows activity starting at ~35-nm at ~0730 that came to within ~2-5-nm of ORD around ~0830-0910 (predawn); the activity then began to dissipate soon after ~0910. The intensity was particularly high at the ~8-20-nm and ~2-3-nm ranges, in part due to the effects range bin areal size relative to storm spatial extent noted previously. Fig. 16 suggests that most of the activity passed just to the S of ORD and then weakened, moving out to ~30-nm range at ~0950 and dissipating by ~1000. Fig 17 showed the activity moved from the S to SE of ORD during this period.

More light activity started to enter the region at a range of 120-nm at ~1100 and continued to come closer to ORD for the next four hours. Fig. 18 shows that this activity passed from the NW to N direction from ORD and then began to recede during this period.

The most extensive activity of the day occurred between ~1800-2400 at ranges from ~2-120-nm. Figs. 16-18 show that this activity consisted of several coherent structures. Fig. 15 shows that these areas consisted of storms approaching and receding from ORD. The most intense activity was ~9-28-nm from ~1850-2140, ~2-10 nm from ~2210-2240 and ~46-54-nm from ~1900-2200. Fig. 16 showed that the activity 30-nm and closer mostly spanned the NW, N through E directions from ~1840-2200 and SW through S and E from ~2200-2400. Fig. 17 showed the activity from 30-60-nm originating from different directions - one from the SW at ~1800 that shifted to the S by ~2010 and then dissipated; another more intense structure from the SW at ~1900 that also moved to the S and dissipated by ~2130; two structures originating ~1820 and ~1950 in the WNW that moved to the N and then easterly (the first appears to have dissipated shortly after 2000 while the second remained intact on to the start of the next day; and a structure that began shortly after 2000 and remained directionally stationary to the E until ~2230. Fig. 18 shows that the most distant storm structures behaved similarly to a great extent. All this activity originated in the SE to S sector and receded away from ORD towards the E as seen from the counterclockwise rotation of azimuth angle with time.

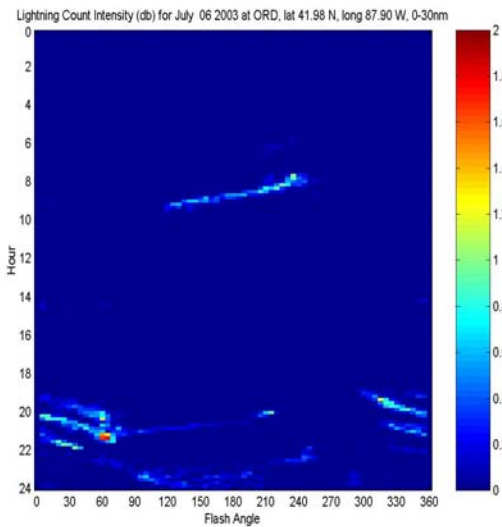


Fig. 16. Azimuth Angle Hovmöller plot: lightning flashes from 0-30-nm of ORD on July 6 2003.

4.2 IAH

Fig. 19 is the distance Hovmöller plot of lightning flashes within 120-nm of IAH. Figs. 20-22 are corresponding azimuth angle plots for the 0-30nm, 30-60-nm and 60-120-nm ranges, respectively.

From ~0000-0310, most of the activity originated in the W and then progressed to the S of IAH as seen in Fig. 20. A second structure became evident between ~40-60-nm at ~0330 in the WNW direction; this structure remained stationary for around 2-hrs. The dominant feature of the day became evident at ~0900 when activity entered the region from the NW throughout

nearly the entire 0-120-nm range with the most intense activity within the ~4-21 nm range. The closest area of activity within that time period started from the W at ~0050 in the ~8-18nm range, expanding to ~2-25nm by ~0150 and continuing until ~0300, then quickly dissipating. There was an increase of intensity as well, first at a range of ~8-15nm at ~0150 and shifted to a ~11-21 nm range by ~0250. This activity generally stayed just W then shifted southward from ~0200-0250. Fig. 20 shows the activity to the WSW at ~0050, then spread out so that it spanned the WSW, W and WNW sectors by ~0150. The area then shifted so that the SW sector was spanned by ~0250. Dissipation was quite abrupt at ~0310 as evident in Figs. 19 and 20.

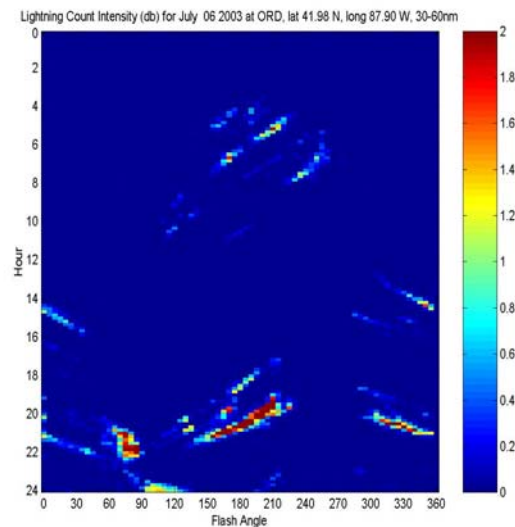


Fig. 17. Azimuth Angle Hovmöller plot: lightning flashes from 30-60-nm of ORD on July 6 2003.

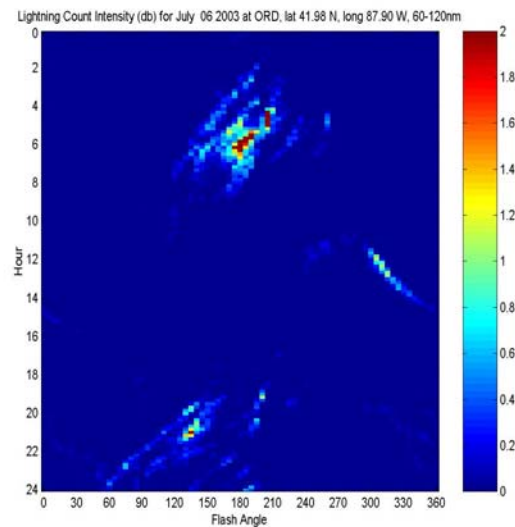


Fig. 18. Azimuth Angle Hovmöller plot: lightning flashes from 60-120-nm of ORD on July 6 2003.

There was another area of somewhat less intense activity at a range of ~30-70nm from ~0310-0620 with the higher intensity activity ~40-52nm from ~0330-0520 and a less intense area at a range of ~55-60nm from ~0330-0420. Fig. 21 shows that this area was confined to the W and WNW sectors then to the W when it dissipated by ~0600.

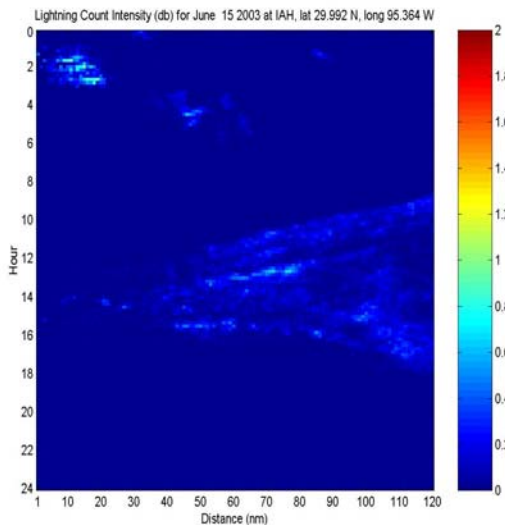


Fig. 19. Distance Hovmöller plot of lightning flashes for IAH on June 15 2003.

The most prominent activity first entered into the 120-nm range from the NW at ~0900 and continued entering defined area of interest through ~1500. The activity moved towards IAH, extending from 60-120-nm away by ~1100, and then extending from ~10-120-nm by 1400. It should be noted that the intensity in the 0-30-nm ranges was considerably less than the 30-60-nm and 60-120-nm ranges, except for isolated areas between ~1400-1500. Fig. 22 shows that, in the range 60-120-nm, activity between ~0900-1800 was from one to at least four different sectors. Fig. 21 indicates that, when lightning activity entered or originated in the 30-60-nm range interval, it was relatively weak, extensive over all sectors and highly coherent in two major directions that approached each other and merged in the SW direction at ~140° azimuth. Fig. 20 shows that most of the activity remained distant from IAH. All the activity that did enter the nearest range interval of 0-30-nm was spread over nearly all azimuth sectors.

5. SUMMARY

This study introduced the application of polar time-distance or Hovmöller plots to lightning data. These plots are well suited to analyzing the behavior of lightning flash activity relative to a fixed observation point. The methodology is demonstrated through use of flash density plots that represent the number of flashes occurring over sequentially equal time periods in areas covered by range bins of equal size out to a prescribed distance from the point of interest. Directional information is obtained by plotting the data as function of azimuthal sectors of a given size. The plots presented

here have a time resolution of 10-min, 1-nm range resolution and 5° angular resolution. Plots were presented for selected days with strong lightning activity near IAH and ORD; average plots for an entire summer season and a one-month period and a one-week period out of this summer were also given. Partitioning of the azimuthal plots for lightning flashes inside 0-30-nm, 30-60-nm and 60-120-nm ranges are shown to facilitate discrimination of storm activity. Characteristics of storm behavior such as onset, decay, duration, intensity, radial and angular velocities may be gleaned from these plots. Although not treated here, the ability to combine temporal and spatial representations of storm activity in various forms, including varying Hovmöller diagrams, spatial portrayals and loop replays of time sequences will be important to better empirical understanding of storm behavior and its governing physics.

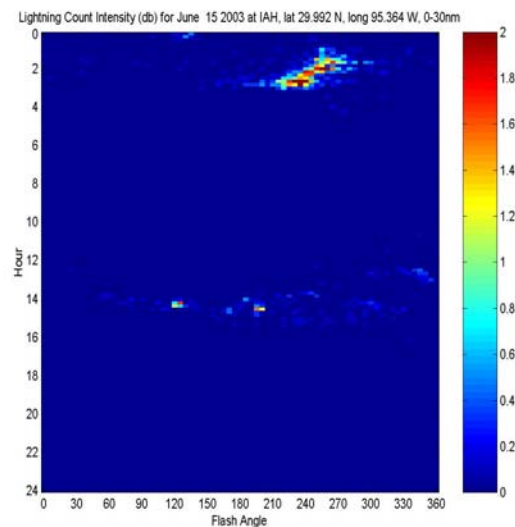


Fig. 20. Azimuth Angle Hovmöller plot of lightning flashes 0-30-nm for IAH on June 15 2003.

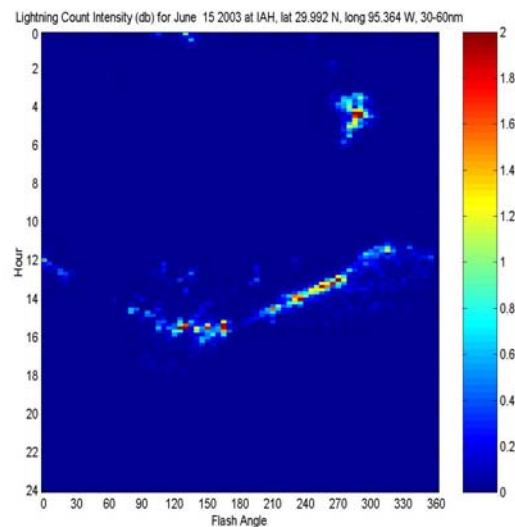


Fig. 21. Azimuth Angle Hovmöller plot of lightning flashes 30-60-nm for IAH on June 15 2003.

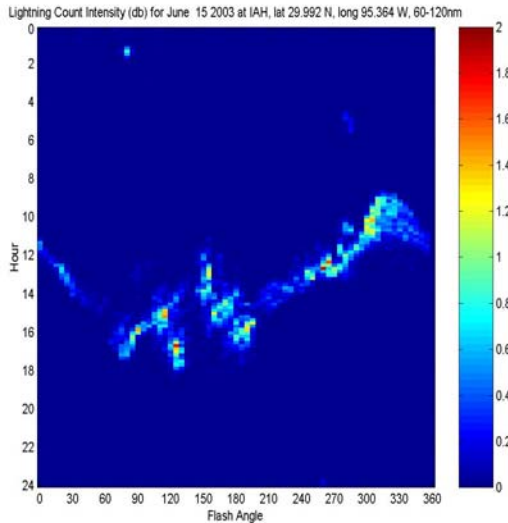


Fig. 22. Azimuth Angle Hovmöller plot of lightning flashes 60-120-nm for IAH on June 15 2003.

6. REFERENCES

- Bates, E. G., T. A. Seliga and T. Weyrauch, 2001: Implementation of grounding, bonding, shielding and power system improvements in FAA systems: Reliability assessments of the Terminal Doppler Weather Radar (TDWR). 20th Digital Avionics Systems Conference, Daytona Beach, FL, 14-18 October.
- Canniff, J. F., 1993: Thunderstorm detection: FAA applications for network lightning data. Preprints 8th Symposium on Meteorological Observations and Instrumentation, AMS Annual Mtg., Anaheim, CA, 91-92.
- Carbone, R. E., J. D. Tuttle, D. A. Ahijevych and S. B. Trier, 2002: Inferences of predictability associated with warm season precipitation episodes. *J. Atmos. Sci.*, **59**, No. 13, 2033–2056.
- Changnon, S. A., 1988a: Climatography of thunder events in the conterminous United States. Part I: Temporal aspects. *J. Climate*, **1**, 389-398.
- Changnon, S. A., 1988b: Climatography of thunder events in the conterminous United States. Part II: Spatial aspects. *J. Climate*, **1**, 399-405.
- Holle, R. L. and R. E. Lopez, 1993: Overview of real-time lightning detection systems and their meteorological uses. NOAA Tech. Memo. ERL NSSL-102, 68 pp.
- Kraus, K. and J. Canniff, 1995: Incorporating lightning data into automated weather observations. Preprints 6th Conference on Aviation Weather Systems, AMS, 466-469.
- Kraus, K., T. A. Seliga and J. R. Kranz, 2000: Final performance evaluation of the Automated Lightning Detection and Reporting System (ALDARS). Preprints 16th International Conference on Interactive Information and Processing Systems (IIPS) for Meteorology, Oceanography, and Hydrology, Long Beach, CA, AMS Annual Mtg., 106-109.
- Orville, R. E., 1991: Lightning ground flash density in the contiguous United States – 1989. *Mon. Wea. Rev.*, **119**, 573-577.
- Orville, R. E. and A. C. Silver, 1997: Lightning ground flash density in the contiguous United States – 1992-95. *Mon. Wea. Rev.*, **125**, 631-638.
- Orville, R. E. and G. R. Huffines, 1999: Lightning ground flash measurements over the contiguous United States: 1995-97. *Mon. Wea. Rev.*, **127**, 2693-2703.
- Orville, R. E. and G. R. Huffines, 2001: Cloud-to-ground lightning in the United States: NLDN results in the first decade, 1989-98. *Mon. Wea. Rev.*, **129**, 1179-1193.
- Rhoda, D. A. and M. L. Pawlak, 1999: An assessment of thunderstorm penetrations and deviations by commercial aircraft in the terminal area. MIT Lincoln Laboratory Project Rept., NASA/A-2, 98 pp.
- Seliga, T. A. and J. A. Shorter, 2000: Contribution to a baseline understanding of the impact of weather on airline carrier operations, Preprints 2nd Symposium on Environmental Applications, AMS Annual Mtg., 9-14 January 2000, Long Beach, CA, 190-193.
- Seliga, T. A., D. A. Hazen and C. Schauland, 2002a: "Comparisons of cloud-to-ground lightning flash data with NEXRAD inferences on rainfall as functions of longitude and latitude". Preprints 6th Symposium on Integrated Observing Systems, American Meteorological Society, Orlando, FL 13-17 January 2002.
- Seliga, T. A., D. A. Hazen and C. Schauland, 2002b: "Analysis of lightning cloud-to-ground flash activity for national aviation choke point region studies". 10th Conference on Aviation, Range, and Aerospace Meteorology, American Meteorological Society, Portland, OR, 13-16 May 2002.